# Spectroscopic Study of Electron and Hole Polarons in a High-Mobility Donor−Acceptor Conjugated Copolymer

Haihua Xu,[†] Yuqian Jiang,[‡] Jun Li,[§] Beng S. Ong,[‖] Zhigang Shuai,[‡] Jianbin Xu,[†] and Ni Zhao*,[†]

[†]Department of Electronic Engineering, The Chinese University of Hong Kong, New Territories, Hong Kong
[‡]Department of Chemistry, Tsinghua University, Beijing, China
[§]Institute of Materials Research and Engineering, Agency for Science, Technology and Research, Singapore
[‖]Department of Chemistry, Hong Kong Baptist University, Kowloon Tong, Kowloon, Hong Kong

ABSTRACT: Recent advances in developing donor−acceptor conjugated copolymers have led to great performance improvement in both organic photovoltaic cells and field-effect transistors. In contrast to the extensive spectroscopic studies on the photoinduced charge transfer and separation processes in these copolymers, little has been done to probe their charge-transport properties on a microscopic scale. In this work, we combine charge modulation spectroscopy (CMS), photoinduced absorption, and chemical doping spectroscopy to interrogate separately the nature of hole and electron transport in a recently developed high-mobility copolymer poly(*N*-alkyl diketopyrrolo-pyrrole dithienylthieno[3,2-b]thiophene) (DPP-DTT). It is found that both hole and electron polarons exhibit two-dimensional delocalization in the DPP-DTT films due to the strong intermolecular coupling. A new subgap charge induced optical transition is observed, which has not been reported before in homopolymers. The origin of this transition is studied by combing the temperature and gate voltage dependent CMS and quantum chemical calculation. The results reveal that this transition could be related to the existence of staggered dimer stacking in copolymers due to the asymmetrical volume fractions of donor and acceptor moieties.
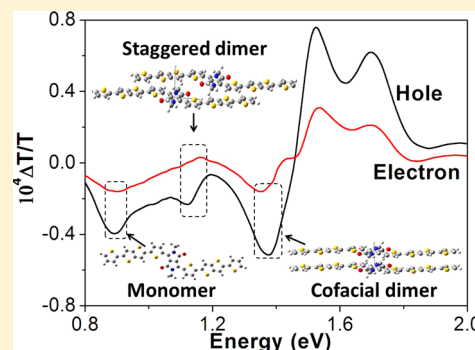
1. INTRODUCTION

In the past decade great progress has been made in improving the electronic properties of conjugated polymers through innovative molecular design. One popular approach is to adopt a backbone structure with alternating electron donor (D) and acceptor (A) repeating moieties. Through π-conjugated, charge transfer from D to A will occur within the backbone, and the extent of charge transfer can be modulated by the donor and acceptor strengths and their interaction. The D−A design has proved especially valuable in manipulating and reducing the bandgap of conjugated polymers,[1] as well as in controlling their charge transport properties.[2,3] High-performance photovoltaic cells (PVs) and field-effect transistors (FETs) have been demonstrated using π-conjugated donor−acceptor copolymers (hereafter referred to as D−A copolymers).[4,5] For the PV application, the impact of the D−A electronic structure on the charge transfer and separation processes has been studied using transient absorption spectroscopy.[6−8] On the other hand, how it affects the charge transport property and the FET performance remains unclear.

Recently, a high molecular weight D−A copolymer, poly(*N*-alkyl diketopyrrolo-pyrrole-dithienylthieno[3,2-b]thiophene) (DPP-DTT), was developed and demonstrated field-effect hole mobility up to 10 cm^{2}V^{-1}s^{-1}.[1] Such remarkable performances are attributed to the properly designed D−A combination, the high molecular weight, and the planar backbone structure, which facilitates formation of a highly ordered and closely packed stacking configuration.[1] In addition, due to the electron-accepting feature of the DPP unit, DPP-DTT also exhibits excellent n-type transport property.[9] To obtain microscopic insights into the nature of charge carries in this interesting material system and to understand how it is affected by the molecular configurations, we herein perform a detailed spectroscopic study on the FET structure of DPP-DTT.

The polaronic nature of charge carriers in organic small molecules and polymers has been investigated using charge modulation spectroscopy (CMS).[10−16] The technique measures the change in the optical transmission spectrum of an FET (or a diode) upon application of a modulated electric field. Characteristic optical signatures of localized and delocalized polarons in molecular semiconductors can be probed; this is in contrast to the chemical doping spectroscopy, by which only localized polarons can be observed. In this work we combine the CMS technique with chemical doping spectroscopy and photoinduced spectroscopy to investigate different transport properties of hole and electron polarons. We have identified for the first time the delocalized polaronic signatures for both electrons and holes. In addition, a new charge-induced absorption feature was observed. Quantum chemical calculations are carried out to interpret these spectral signatures.
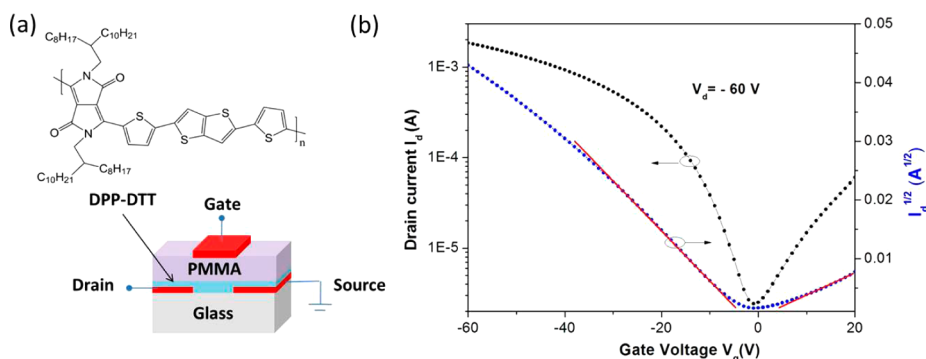
Figure 1. (a) Schematic configuration of a DPP-DTT top-gate FET (dielectric layer: PMMA) (channel length, 50 μm; channel width, 9 mm). (b) Transfer characteristics of the FET (drain-source voltage: $V_d = -60$ V).

2. EXPERIMENTAL METHODS

To perform the CMS measurements, a semitransparent top-gate, bottom-contact FET structure was used (Figure 1a). Gold source-drain electrodes with a thickness of 15 nm were defined by photolithography on a glass substrate. The surface of the gold electrodes was modified with a 10 mM solution of 1-octanethiol in isopropyl alcohol for 2 min at room temperature to improve the morphology of DPP-DTT. The semiconductor film was then deposited by spin-coating a 4 mg/mL solution of high molecular weight DPP-DTT copolymer (the average molecular weights (M_n/M_w) were 110 000/501 000) in 1,2-dichlorobenzene and annealed at 135 °C for 30 min in a nitrogen atmosphere. To fully dissolve DPP-DTT, the polymer solution was heated at 90 °C for 15 min, followed by quenching the solution in an ice bath in an ultrasonicator for 10 min. Subsequently, a 540-nm-thick dielectric layer of PMMA was spin-coated on the semiconductor film and annealed at 80 °C for 30 min. Finally, a semitransparent aluminum gate electrode was deposited on the dielectric layer.

In the CMS experiment, the FET device is placed inside a cryostat that allows measurements in vacuum ($<10^{-5}$ mbar) at various temperatures. A voltage bias consisting of a dc and a small ac component (4 V) is applied on the gate of the FET to induce charge carriers. During bias the device is probed with a monochromatic light beam generated by a halogen lamp and a double-grating monochromator. The transmitted probe light is detected by either Si (visible) or Ge (infrared) photodiodes, and the electrical signal is then fed into a Stanford SR530 lock-in amplifier (using the ac modulation frequency as its reference). The charge-induced absorption is determined as the ac voltage modulated transmission ΔT divided by the total transmission T through the unbiased device. The normalized quantity $\Delta T/T$ is displayed with its X (in phase) and Y (quadrature) components, and the phase of the signal is determined by $\tan^{-1}(Y/X)$. The capacitance–voltage characteristics were taken with an impedance analyzer. A parallel resistor–capacitor circuit model was used to calculate the capacitance values from the measured complex impedance Z.

3. RESULTS AND DISCUSSION

A. Spectroscopic Studies on the Nature of Hole and Electron Transport.
Figure 1b shows the ambipolar transfer characteristics of a typical CMS testing device, exhibiting room temperature hole and electron saturation mobilities of 1.72 and 0.42 cm^{2}V^{-1}s^{-1}, respectively. It is worth mentioning that the device structure used in this study was optimized for the CMS measurement and therefore yields mobility values lower than

those reported in ref 1. Nevertheless, they are still within the high mobility regime (>0.1 cm^{2}V^{-1}s^{-1} for electron mobility and >1 cm^{2}V^{-1}s^{-1} for hole mobility) and should manifest the same charge transport characteristics. Similar to the previous report,[1] we observed nearly an order difference between the electron and hole mobility. This could be due to electron polarons being highly localized and/or the existence of a relatively large number of deep electron traps at the semiconductor/dielectric interface.[17] To elucidate whether the asymmetric transport is dominated by the polaronic effect or energetic disorder,[14,18] we first performed the CMS measurements on a device in both p-type and n-type transport regimes.

The typical hole and electron CMS spectra of a DPP-DTT FET measured in accumulation are shown in Figure 2b. The measurements were taken at room temperature with a
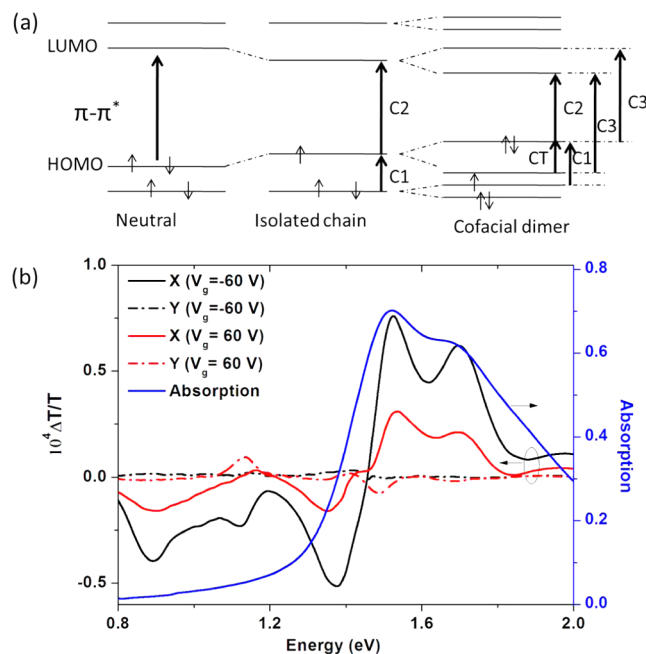
Figure 2. (a) Energy-level diagram and possible optical transitons for neutral polymer (left), hole polarons on a single chain (middle), and hole polarons delocalized over two cofacial chains (right) (CT, charge transfer). (b) CMS spectra of DPP-DTT FETs in the hole and electron accumulation regions and the absorption spectrum of a pure DPP-DTT thin film. In the CMS measurements, a modulation voltage of ±4 V was used, and the dc gate bias voltages for hole and electron accumulation were −60 and 60 V, respectively.
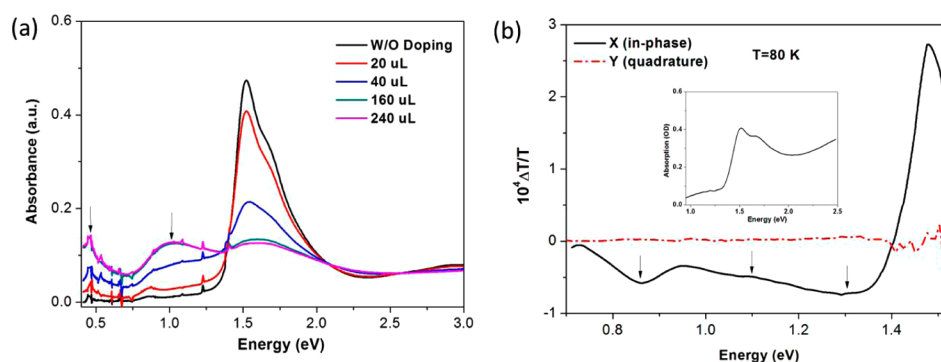
Figure 3. (a) Chemical doping spectra of DPP-DTT in a dilute chloroform solution. (1×10^{-5} M). The oxidative reagent (1×10^{-3} M FeCl$_3$ chloroform solution) was added gradually. (b) Photoinduced absorption spectrum of a DPP-DTT/PCBM (1:4 by weight) blended thin film at 80 K. Inset: absorption spectra of DPP-DTT/PCBM blended thin film.
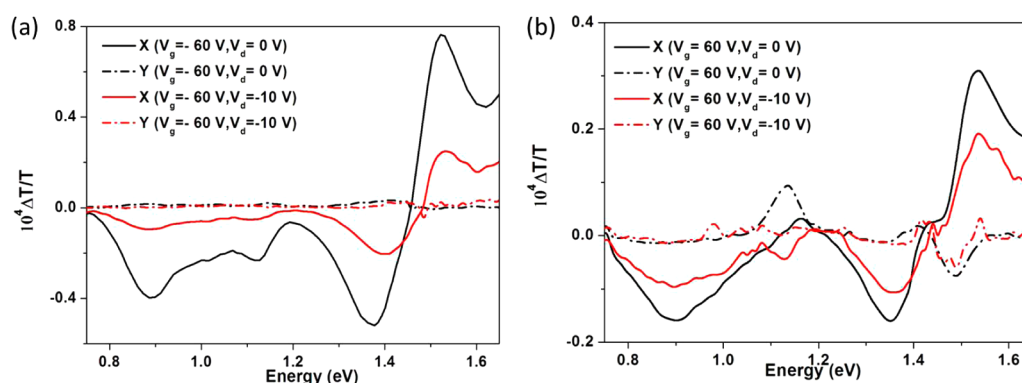

Figure 4. Lateral electric field dependent CMS spectra from (a) hole accumulation and (b) electron accumulation (black lines, $V_d = 0$ V; red lines, $V_d = -10$ V) with a modulation frequency of 200 Hz at room temperature.

modulation frequency of 200 Hz and source-drain bias of 0 V. Between 1.5 and 2.0 eV both hole and electron CMS spectra exhibit a characteristic bleaching ($\Delta T/T > 0$) of $\pi - \pi^*$ absorption due to removal of neutral polymer segments upon charge injection. Below 1.5 eV is the charge-induced absorption ($\Delta T/T < 0$) region with two main absorption peaks centered around 0.88 and 1.38 eV. Such doublet optical transitions are quite similar with those observed in high-mobility homopolymers, such as poly(3-hexylthiophene) (P3HT) and poly(2,5-bis(3- tetradecylthiophen-2-yl)thieno[3,2-b]thiophene) (pBTTT).[1,15,16] According to the previous studies, the feature at 0.88 eV may be assigned to the absorption of the polarons localized on an isolated chain (C2 transistion in Figure 2a), whereas the peak at 1.38 eV would be a manifestation of the delocalized interchain nature of polarons in the two-dimensional conjugated lamellae of polymer chains (C3 transistion in Figure 2a). Besides the absorption peaks at 0.88 and 1.38 eV, we also observed an additional feature at 1.11 eV (in the x-channel for the p-type region and y-channel for the n-type region). The origin of this feature will be discussed in the next section.

To further verify the physical origins of the charge-induced subgap absorption, we measured the chemical doping spectra of isolated charged polymer chains in very dilute DPP-DTT solution (1×10^{-5} M). When gradually adding the oxidative dopant FeCl$_3$ to the neutral DPP-DTT solution, the characteristic HOMO−LUMO absorption of DPP-DTT at around 1.4−2.0 eV was bleached, and the charge-induced absorptions started to appear at 0.4 and 0.95 eV (shown in Figure 3a). Considering that in the chemical doping spectra of solution

only the optical transitions of the isolated charged chains can be observed, we can assign the two absorption features as then C1 and C2 transitions (shown in Figure 2a). Compared to the C2 peak at 0.88 eV in the CMS spectra, the C2 transition in the chemical doping spectra is slightly blue-shifted. This is likely due to the reduction of the conjugation length of the polymer chains as they adopt a more twisted configuration in the solution phase.[13] We also note that the positions of the C1, C2, and C3 peaks observed in the CMS and chemical doping spectra obey the relation C1 + C2 ≈C3, an empirical equation that has been experimentally valided in P3HT.[10] On the basis of these results, we can confirm our assignment of the subgap CMS features to the C2 and C3 transitions.

One important result revealed by the CMS spectra (in Figure 2b) is that the C3 transition exists for both hole and electron polarons. This differs from the previous results obtained in low-mobility ambipolar homopolymers, where the C3 transition exists merely in the hole accumulation region.[5,11] Such difference provides clear spectroscpic evidence that, in ambipolar polymers with sufficiently high hole or electron mobilities (typically >0.1 cm^{2}V^{-1}s^{-1}), both positively and negatively charged carriers could exhibit two-dimensional delocalization. Similar to the previous studies, we can take the intensity ratio of C3/C2 as a measure of the degree of interchain polaron delocalization.[10,14,19,20] It can be seen that the C3/C2 ratio of the negative polarons is lower than that of the positive polarons, indicating a weaker interchain delocalization of electrons in DPP-DTT thin films. This result is consistent with the observation that the electron mobility (0.42 cm^{2}V^{-1}s^{-1}) is significantly lower than the hole mobility (1.72
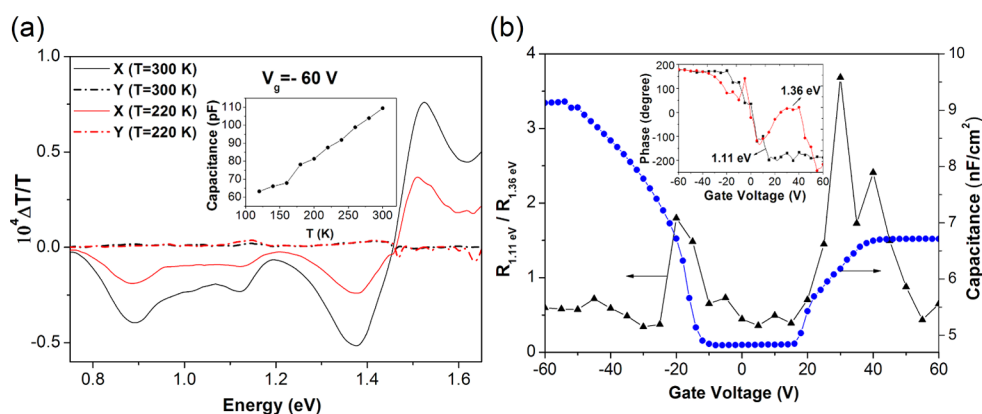
Figure 5. (a) Temperature-dependent CMS spectra from hole accumulation (black lines, 300 K; red lines, 220 K) with a modulation frequency of 200 Hz. Inset: capacitance vs temperature curve at $V_g = -60$ V. (b) The gate-dependent intensity ratio of 1.11 and 1.38 eV (black line) and the capacitance−voltage ($C−V$) characteristics (blue line). Inset: The CMS phase signals of 1.11 and 1.38 eV features at different gate voltages.
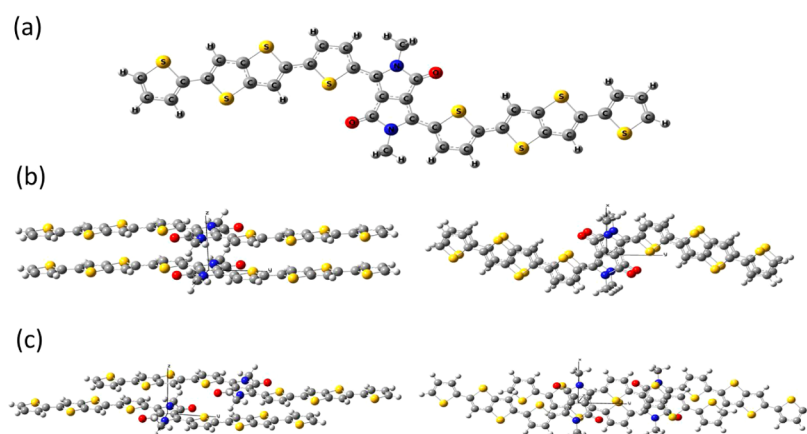
Figure 6. Schematic representation of the shapes and geometries of the DFT-calculated (a) neutral, (b) cofacial dimer, and (c) staggered dimer of DTT-DPP-DTT.

$cm^2V^{-1}s^{-1}$) in the DPP-DTT FETs. Nevertheless, we still expect that the energetic disorder plays a more doninant role (than polaronic effect) in determining the charge transport properties of the DPP-DTT devices. The drain voltage dependent CMS spectra (Figure 4) were also measured. The result shows little change of the C3/C2 ratio at different drain voltages, suggesting that the lateral electric field has a weak influence on the interchain delocalization of polarons.

B. Origin of the 1.11 eV Subgap Optical Transition. Now we turn to discuss the origin of the subgap feature that appears around 1.11 eV in the CMS spectra. Such feature has not been observed previously in homopolymer systems. As shown in Figure 2b, the charge-induced absorption at 1.11 eV appears in the X-channel for the p-type region and in the Y-channel for the n-type region. Note that the CMS measurement yields both the in-phase (X) and quadrature (Y) signals and that a nonzero Y component would indicate a phase difference between different electronic processes. Consequently, the phase change of the 1.11 eV transition suggests that it may originate from a process that is different from the C2 and C3 transitions of polarons. To elucidate this point, we first checked whether the 1.11 eV feature is caused by the interference effect and/or the electroabsorption of the FET structure in the CMS measurements. Photoinduced absorption (PIA) spectroscopy was performed on a DPP-DTT/PCBM blend film at 80 K using a modulated pump laser (635 nm) with a frequency of

200 Hz. The obtained spectrum is shown in Figure 3b, which exhibits the bleaching neutral $\pi−\pi^*$ transition around 1.50 eV, photoinduced subgap absorption peaks centered at 0.89 eV, 1.36 eV, and a pronounced shoulder centered around 1.1 eV. Such photoinduced absorption features resemble the CMS results, although the peaks in the PIA spectrum are broadened, possibly due to the lower degree of ordering of DPP-DTT molecules in the blend film. In the PIA measurement the possible electric field induced absorptions due to the FET structure and the gate dielectric effects are eliminated; therefore, we can confirm from the PIA results that the subgap absorption at 1.11 eV originates from charge species within the DPP-DTT film.

Next, we consider the possibility that the 1.11 eV feature is related to bipolarons. Several observations suggest this an unlikely assignment. For long-chain molecules with low doping levels, the increase in configurational entropy would favor the dissociation of bipolarons to polarons through the $BP^\pm \rightarrow P^\pm + P^\pm$ process.[21,22] Therefore the bipolaron to polaron ratio should increase at low temperatures or at high carrier concentration. Accordingly, if the 1.11 eV feature corresponds to bipolaons, its intensity relative to the C2 and C3 peaks should increase in these conditions. To check this assumption, we first compare the CMS spectra taken at 300 and 220 K (Figure 5a). According to the polaron models developed by Frohlich and Holstein, the charge transports between adjacent molecules are
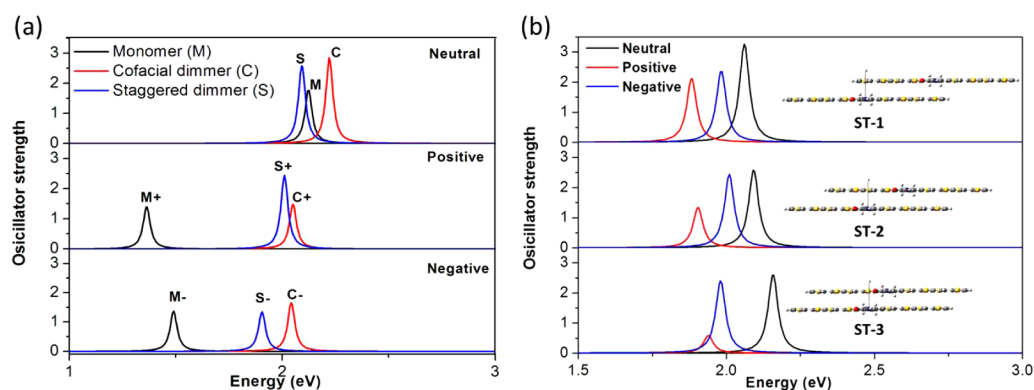
Figure 7. (a) Calculated absorption spectra of the neutral and singly charged monomers (black dashed line), cofacial (red dashed line), and staggered (blue dashed line) dimers. (b) Calculated absorption spectra of the neutral (black dashed line), positive (red dashed line), and negative (blue dashed line) staggered dimers with different staggered configurations.

thermally activated by sufficiently high temperatures;[23−25] thus, all the charge-induced bleaching and absorption features will have reduced intensity at low temperatures. This is confirmed in Figure 5a and is consistent with capacitance−voltage characteristics at different temperatures (inset of Figure 5a). Importantly, the signal of the 1.11 eV feature reduces together with the C2 and C3 peaks, and there is no significant change in the ratio of the peak intensity. This result is inconsistent with the assginment of the 1.11 eV feature to bipolarons.

Furthermore, we compared the ratio of the $\Delta T/T$ values at 1.11 and 1.36 eV (C3 peak) at different gate voltages. To eliminate the effect of the phase difference, we used the amplitude values of the signal to calculate the ratios. As shown in Figure 5b, the ratio of the 1.11 eV feature over the C3 peak does not increase at high gate voltages, that is, at high hole/electron carrier concentration. This, again, suggests that the 1.11 eV feature is not related to bipolarons. Interestingly, at low carrier concentration the 1.11 eV feature is enhanced as compared to the C3 transition, indicating that (1) the feature may be associated with a bulk state and (2) the state corresponds to the least energetic unoccupied state where injected charges will first fill in.

C. Quantum Chemical Calculations. To gain further insight into the CMS results, we calculated the electronic structures of neutral and charged DPP-DTT monomers in both single-chain and dimer configurations using the TDDFT method at the CAM-B3LYP/6-31+G(d) level as implemeted in GAUSSIAN 09.[26] We chose the symmetric DTT-DPP-DTT configuration (Figure 6a) as the model monomer system to stabilize the donor−acceptor complex during calculation.[27,28] The geometries of the neutral and charged monomers are optimized using B3LYP/6-311++G(d,p) by keeping a planar configuration. In the case of the dimer structure, we consider two configurations: cofacial dimer (Figure 6b) and staggered dimer (Figure 6c). In the cofacial configuration the DTT and DPP units of the two adjacent monomors are well aligned respectively (Figure 6b). In the staggered dimer, on the other hand, one monomor is translated along the backbone direction with respect to the other, such that the neighboring DTT and DPP units are no longer aligned to each other (Figure 6c). The cofacial and staggered dimers are formed by putting two optimzed monomers together without optimization. The interchain distance of the dimers is set on the order of 3.43 Å.[1] Although the DTT-DPP-DTT structure used here cannot represent the exact electronic structure of the DPP-DTT

polymer system, it contains the key D and A components and should help us to qualititively understand the spectroscopic features observed experimentally.

Figure 7a shows the calculated linear absorption spectra of the neutral and singly charged monomers and dimers. In the top panel the three peaks at 2.12, 2.09, and 2.22 eV originate from the absorption of the neutral monomer (M), staggered dimer (S), and cofacial dimer (C), respectively. The middle and bottom panels display the absorption spectra of the positively and negatively charged polarons. In both spectra the charged monomers (M+, M−) and cofacial dimers (C+, C−) exhibit the absorption peaks with the lowest and highest excitation energies, respectively, and the staggered dimers (S+, S−) are responsible for the absorption peaks appearing in the middle. Figure 7b illustrates that the position of the middle peak will vary depending on the translation distance between the adjacent molecules in the staggered dimer.

Now we can further discuss the experimental CMS data in light of the simulation results. Since the use of monomer in the simulation reduces the conjugation length of the DPP-DTT system, the calculated absorption peaks are blue-shifted by 0.5− 0.8 eV compared to the experimental results. Nevertheless, we can correlate each calculated peak with the measured CMS features. First, with some broadening the nearly overlapped S and M peaks could merge into one peak with a stronger intensity compared to the higher energy C peak. This is consistent with the shape of the doublet bleaching signal measured in the CMS experiments. Second, the relative peak positions of the charged monomers (M+, M−) and cofacial dimers (C+, C−) agree well with the C2 and C3 positions in the CMS spectra. Third, the simulation results predict that the staggered dimer configuration could introduce an intermediate charge-induced absorption feature between C2 and C3. According to the gate voltage dependent measurement, the staggered dimer may provide the lowest energy state where charge carriers will preferentially fill in. It is important to point out that the exact position of absorption peaks of the charged staggered dimer should depend on the translation distance between the adjacent molecules of the dimer as well as the torsion angle of the backbone. Here we demonstrate a simplified senario with zero torsion angle and a few different translation distances. A more thorough quantum chemical calculation study would be needed to verify if a better agreement can be achieved between the theoretical and experimental results.

4. CONCLUSIONS

In summary, we have carried out a systematic spectroscopic study on the polaronic nature of charge carriers in a newly developed donor−acceptor copolymer system, DPP-DTT. This material system exhibits excellent ambipolar charge transport property with the electron and hole mobility exceeding 0.1 and 1 cm^{2}V^{-1}s^{-1}, respectively. Accordingly, we observed the delocalized polaronic signatures for both electrons and holes in the CMS measurement. The similarity between the electron and hole CMS spectra suggests that the large difference between electron and hole field-effect mobility is likely due to the energetic disorder, rather than the polaronic effect. A new charge-induced absorption feature between the C2 and C3 peaks are observed, which has not been seen before in homopolymer systems. The PIA and the temperature and gate voltage dependent CMS measurements show that the feature is not associated with bipolaron, electroabsorption, or gate dielectric effect. The increase in its relative amplitude at smaller biases suggests that it could behave like a shallow trap state. According to the quantum chemical calculations, this state may be related to the existence of staggered dimer configuration. Our combination of spectroscopic and theoretical studies should lead to better molecular-scale understanding of the electronic structure and the charge transport process in donor−acceptor copolymer systems that promise high performance for not only FETs but also organic photovoltaic cells.

■ AUTHOR INFORMATION

Corresponding Author
*nzhao@ee.cuhk.edu.hk.

Notes
The authors declare no competing financial interest.

■ ACKNOWLEDGMENTS

■ REFERENCES

(1) Li, J.; Zhao, Y.; Tan, H. S.; Guo, Y. L.; Di, C.; Yu, G.; Liu, Y. Q.; Lin, M.; Lim, S. H.; Zhou, Y. H.; et al. A Stable Solution-Processed Polymer Semiconductor with Record High-Mobility for Printed Transistors. *Sci. Rep.* **2012**, *2* (754), 1−9.

(2) Li, Y.; Sonar, P.; Singh, S. P.; Soh, M. S.; Meurs, M.; Tan, J. Annealing-Free High-Mobility Diketopyrrolopyrrole-Quaterthiophene Copolymer for Solution-Processed Organic Thin Film Transistors. *J. Am. Chem. Soc.* **2011**, *133*, 2198−2204.

(3) Li, Y.; Singh, S. P.; Sonar, P. A High Mobility P-Type DPP-Thieno[3,2-b]thiophene Copolymer for Organic Thin-Film Transistors. *Adv. Mater.* **2010**, *22*, 4862−4866.

(4) Mondal, R.; Ko, S.; Bao, Z. Fused Aromatic Thienopyrazines: Structure, Properties and Function. *J. Mater. Chem.* **2010**, *20*, 10568−10576.

(5) Zhang, X. R.; Richter, L. J.; DeLongchamp, D. M.; Kline, R. J.; Hammond, M. R.; McCulloch, I.; Heeney, M.; Ashraf, R. S.; Smith, J. N.; Anthopoulos, T. D.; et al. Molecular Packing of High-Mobility Diketo Pyrrolo-Pyrrole Polymer Semiconductors with Branched Alkyl Side Chains. *J. Am. Chem. Soc.* **2011**, *133*, 15073−15084.

(6) Nogueira, A. F.; Montanari, I.; Nelson, J.; Durrant, J. R.; Winder, C.; Sariciftci, N. S.; Brabec, C. Photoinduced Carrier Generation in P3HT/PCBM Bulk Heterojunction Materials. *J. Phys. Chem. B* **2003**, *107*, 1567−1573.

(7) Bakulin, A. A.; Hummelen, J. C.; Pshenichnikov, M. S.; van Loosdrecht, P. H. M. Ultrafast Hole-Transfer Dynamics in Polymer/ PCBM Bulk Heterojunctions. *Adv. Funct. Mater.* **2010**, *20*, 1653−1660.

(8) Guo, J.; Ohkita, H.; Benten, H.; Ito, S. Bimodal Polarons and Hole Transport in Poly(3-Hexylthiophene):Fullerene Blend Films. *J. Am. Chem. Soc.* **2010**, *132*, 9631−9637.

(9) Guo, X.; Zhang, M. J.; Tan, J. H.; Zhang, S. Q.; Huo, L. J.; Hu, W. P.; Li, Y. F.; Hou, J. H. Influence of D/A Ratio on Photovoltaic Performanceof a Highly Efficient Polymer Solar Cell System. *Adv. Mater.* **2012**, *24*, 6536−6541.

(10) Sirringhaus, H.; Brown, P. J.; Friend, R. H.; Nielsen, M. M.; Bechgaard, K.; Langeveld-Voss, B. M. W.; Spiering, A. J. H.; Janssen, R. A. J.; Meijer, E. W.; Herwig, P.; et al. Two-Dimensional Charge Transport in Self-Organized, High-Mobility Conjugated Polymers. *Nature* **1999**, *401*, 685−688.

(11) Chen, Z.; Bird, M.; Lemaur, V.; Radtke, G.; Cornil, J.; Heeney, M.; McCulloch, I.; Sirringhaus, H. Origin of the Different Transport Properties of Electron and Hole Polarons in an Ambipolar Polyselenophene-Based Conjugated Polymer. *Phys. Rev. B* **2011**, *84* (115211), 1−14.

(12) Brown, P. J.; Sirringhaus, H.; Harrison, M.; Shkunov, M.; Friend, R. H. Optical Spectroscopy of Field-Induced Charge in Self-Organized High Mobility Poly(3-Hexylthiophene). *Phys. Rev. B* **2001**, *63* (125204), 1−11.

(13) Deng, Y. Y.; Sirringhaus, H. Optical Absorptions of Polyfluorene Transistors. *Phys. Rev. B* **2005**, *72* (045207), 1−12.

(14) Zhao, N.; Noh, Y.-Y.; Chang, J. F.; Heeney, M.; McCulloch, I.; Sirringhaus, H. Polaron Localization at Interfaces in High-Mobility Microcrystalline Conjugated Polymers. *Adv. Mater.* **2009**, *21*, 3759−3763.

(15) Caironi, M.; Bird, M.; Fazzi, D.; Chen, Z.; Di Pietro, R.; Newman, C.; Facchetti, A.; Sirringhaus, H. Very Low Degree of Energetic Disorder as the Origin of High Mobility in an n-Channel Polymer Semiconductor. *Adv. Funct. Mater.* **2011**, *21*, 3371−3381.

(16) Kim, M. G..; Kanatzidis, M. G.; Facchetti, A.; Marks, T. J. Low-Temperature Fabrication of High-Performance Metal Oxide Thin-Film Electronics via Combustion Processing. *Nat. Mater.* **2011**, *10*, 382−388.

(17) Murphy, A. R.; Fréchet, J. M. Organic Semiconducting Oligomers for Use in Thin Film Transistors. *Chem. Rev.* **2007**, *107*, 1066−1096.

(18) Chang, J. F.; Sirringhaus, H.; Giles, M.; Heeney, M.; McCulloch, I. Relative Importance of Polaron Activation and Disorder on Charge Transport in High-Mobility Conjugated Polymer Field-Effect Transistors. *Phys. Rev. B* **2007**, *76* (205204), 1−12.

(19) Sirringhaus, H. Device Physics of Solution-Processed Organic Field-Effect Transistors. *Adv. Mater.* **2005**, *17*, 2411−2425.

(20) Beljonne, D.; Cornil, J.; Sirringhaus, H.; Brown, P. J.; Shkunov, M.; Friend, R. H.; Brédas, J.-L. Optical Signature of Delocalized Polarons in Conjugated Polymers. *Adv. Funct. Mater.* **2001**, *11*, 229−234.

(21) Nowak, M. J.; Spiegel, D.; Hotta, S.; Heeger, A. J.; Pincus, P. A. Charge Storage on a Conducting Polymer in Solution. *Macromolecules* **1989**, *22*, 2917−2926.

(22) Ziemelis, K. E.; Hussain, A. T.; Bradley, D. D. C.; Friend, R. H.; Rühe, J.; Wegner, G. Optical Spectroscopy of Field-induced Charge in Poly (3-hexyl thienylene) Metal-Insulator-Semiconductor Structures: Evidence for Polarons. *Phys. Rev. Lett.* **1991**, *66*, 2231−2234.

(23) Fröhlich, H.; Pelzer, H.; Zienau, S. XX. Properties of Slow Electrons in Polar Materials. *Philos. Mag.* **1950**, *41*, 221−242.

(24) Holstein, T. Studies of Polaron Motion: Part I. The Molecular-Crystal Model. *Ann. Phys.* **1959**, *8*, 325−342.

(25) Holstein, T. Studies of Polaron Motion: Part II. The "Small" Polaron. *Ann. Phys.* **1959**, *8*, 343−389.

(26) Frisch, M. J.; Trucks, G. W.; Schlegel, H. B.; et al. *GAUSSIAN 09*, Revision A.1; Gaussian, Inc.: Wallingford, CT, 2009.

6840

dx.doi.org/10.1021/jp4003388 | *J. Phys. Chem. C* 2013, 117, 6835−6841

(27) Beaujuge, P. M.; Amb, C. M.; Reynolds, J. R. Spectral Engineering in π-Conjugated Polymers with Intramolecular Donor-Acceptor Interactions. *Acc. Chem. Res.* **2010**, *43*, 1396−1407.

(28) Khlyabich, P. P.; Burkhart, B.; Ng, C. F.; Thompson, B. C. Efficient Solar Cells from Semi-Random P3HT Analogues Incorporating Diketopyrrolopyrrole. *Macromolecules* **2011**, *44*, 5079−5084.

6841

dx.doi.org/10.1021/jp4003388 | *J. Phys. Chem. C* 2013, 117, 6835−6841